Continuous Symmetry Measures: Finding the Closest C_2-Symmetric Object or Closest Reflection-Symmetric Object Using Unit Quaternions

YAIR SALOMON, DAVID AVNIR

Institute of Chemistry and the Lise Meitner Minerva Center for Computational Quantum Chemistry, Hebrew University of Jerusalem, Jerusalem 91904, Israel

Received 11 August 1998; accepted 23 November 1998

ABSTRACT: A closed-form solution is provided for the problem of finding the closest reflection-symmetric object, and its relation to the problems of finding the closest achiral object, the closest inversion-symmetric object, and the closest projection plane is discussed. The key to the solution is reducing this problem to the problem of finding the best (least squares) c_2 rotation between two sets of points, in addition to solving the problem of finding the closest C_2-symmetric object. The solution is derived using the quaternion representation of rotation. It is shown that calculation of the best c_2 rotation can be reduced to the diagonalization of the outer product matrix of the pair (between the two sets).
 J Comput Chem 20: 772–780, 1999

Keywords: symmetry; chirality; rotation; C_2-axias; inversion; reflection; quaternions

Introduction

Although symmetry serves as a central tool in the understanding of molecular behavior, symmetric molecules are the exception rather than the rule. Not only do most of the known $\sim 18*10^6$ molecules possess only a C_1 element, but, when dynamics is taken into account, even molecules classically treated as symmetric lose this symmetry, provided a fine enough temporal resolution is used for observation. The dichotomy of using a descriptive tool that conforms with reality only in an approximate way has led to interest in the quantitative assessment of deviations from symmetry and to the closely related quantitative evaluation of achirality. An early example of the use of symmetry as a measurable parameter was done by King et al.[1] who analyzed the spectrum of an asymmetric rigid rotor using Ray's asymmetry parameter.[2] Ray's parameter relates, however, to the

*Correspondence to: D. Avnir; e-mail: david@chem.ch.huji.ac.il

 CCC 0192-8651 / 99 / 080772-09

deviation of the rotor from being prolate or oblate and is not a symmetry parameter in the strict sense of relating to a symmetry group. In two recent reviews,[3] we discussed later propositions for approaching this problem, both for symmetry in general and for achirality as a special case, and the interested reader is referred to these publications. (Also, a small selection of relevant studies is collected in ref. 4.)

The approaches we developed[5]—the continuous symmetry measure (CSM) and the special case of continuous chirality measure (CCM)[6]—provide an explicit way of calculating the distance between an object (in most applications, the vertices of which are the nuclei of a molecule) and the closest (by the normalized sum of squares) G-symmetric object, defined as:

$$S(G) = \frac{1}{N \cdot d} \sum_{j=1}^{N} (p_j - \hat{p}_j)^2 \qquad (1)$$

where G is a specified symmetry group and d is the r.m.s. distance of p_j from the center of mass, and

$$\{ p_j \}_{j=1}^{N}$$

is the set of N points modeling the object, and:

$$\{ \hat{p}_j \}_{j=1}^{N}$$

is the closest G-symmetric object. All of our previous applications related to point of equal weight, but this measure can be easily generalized to give different weights ω_j to different points:

$$S(G) = \sum \omega_j (p_j - \hat{p}_j)^2$$

Without losing generality, we use, in what follows, a previously normalized object:

$$\frac{1}{N} \sum p_j^2 = 1$$

The procedure for the calculation of:

$$\{ \hat{p}_j \}_{j=1}^{N}$$

the so-called ''folding–unfolding procedure'' was originally applied in two dimensions (2D) and then extended to 3D for several cases.[5–8] When G is an achiral group, $S(G)$ measures the degree of chirality (the CCM), provided G gives the minimal $S(G)$ out of all achiral groups; in the majority of cases, G is the group composed of the identity and reflection (σ) elements. CSM and CCM analyses have been applied successfully to a variety of symmetry and chirality problems in chemistry.[9,10] It should be noted that the study of the distance from reflection symmetry and from achirality are distinctly different issues that may, but need not, coincide. Both measures are valuable and may cater to different applications. One of the aims of this article is to emphasize the difference between the two measures and to provide a proper tool for the former.

A difficulty with the folding–unfolding procedure of the CSM methodology in 3D is that it does not specify explicitly the orientation of the symmetry elements. Thus, to find the optimal G-symmetric object, one must calculate the optimal orientation of the symmetry elements, either iteratively (by some minimization recipe) or by closed-form solution. Closed-form solutions are desirable and such solutions for the two most commonly used symmetries, C_2 symmetry and reflection symmetry, are the main focus of this work. The importance of reflection symmetry—in fact, of the study of lack of it—need not be reiterated. C_2 symmetry is, likewise, of major interest, particularly in biology and biochemistry. Interestingly, many of these biosystems are only close to being C_2 symmetric, and hence the need to evaluate quantitatively the content of this symmetry. Examples we analyzed recently, using the CSM approach, include the near C_2 symmetry of the photosynthetic reaction center and that of the HIV-protease.[10]

We begin with a general discussion of procedures for the calculation of the closest achiral object, using solutions to the pose estimation problem; that is, finding the best superpositioning of two sets of points.[11–13] (This problem has been of special interest in the field of robotics and image processing.[12,13]) We then make clear distinction between several problems: finding the closest reflection-symmetric object; finding the closest achiral object; finding the closest inversion-symmetric object; and finding the closest projection plane. Some of these distinctions have been overlooked in our earlier work.[6] We then analyze the first of these problems, namely finding the closest reflection-symmetric object, and provide—to the best of our knowledge, for the first time—a closed-form solution. The key to the solution is the reduction of the problem to the finding of the best (by least squares) c_2 rotation between two sets of points, which leads also to solution of the problem of finding the closest C_2-symmetric object. The solu-

tion is derived using the quaternion representation of rotation and it is shown that the calculation of the best c_2 rotation can be reduced to the diagonalization of the pair's outer product matrix (between the two sets).

The Problem: Finding Closest Reflection-Symmetric Object

The problem of finding the closest achiral object is distinctly different from the problem of finding the closest reflection-symmetric object, the latter of which is our present concern. It is essential to clarify the distinction between these two concepts, which may or may not coincide. The measurement of chirality is in fact a measure of achirality; that is, one evaluates the distance of the chiral object from the nearest achiral configuration. That nearest configuration may be mirror symmetric, inversion symmetric, or symmetric toward higher improper elements, S_n. Although quite often the nearest achiral configuration is mirror symmetric, this need not be the case, and, in principle, one should screen over all S_n values, to locate the minimal $S(S_n)$, which then becomes the chirality measure. The problem we are treating here is different: finding the nearest mirror-symmetric object, whether or not it coincides with the closest achiral object. In what follows, we recall the procedure for determination of distance to achirality.

Several propositions for measuring chirality, including our CCM methodology, are based on finding the optimal congruence; that is, the optimal overlapping positioning of the two enantiomers. Figure 1 illustrates the general scheme of our method (see ref. 14 for a review of various methods). Measuring the distance between the two enantiomeric sets by the mean sum of squares (MS) ensures that the closest achiral object is determined by the average between the two. The use of MS has other more fundamental advantages, such as giving the most probable achiral configuration.[8] The optimal congruence that is pursued is between pairs of points, each composed of a point of one enantiomer and a point of the reflected enantiomer. An obvious constraint is that this pairing must be of equivalent points. For instance, we assume that the points in Figure 1 all represent the same type of atom, then, as seen in Figure 1, some of the points are paired to their own enantiomeric reflections ($2 \leftrightarrow 2'$, $4 \leftrightarrow 4'$, $6 \leftrightarrow 6'$, $8 \leftrightarrow 8'$), whereas others are paired to different, but equivalent, enantiomeric reflections ($1 \leftrightarrow 3'$, $3 \leftrightarrow 1'$, $5 \leftrightarrow 7'$, $7 \leftrightarrow 5'$). The object and its enantiomer have the same logical graph and therefore it is sometimes more convenient to study the possible pairings as internal pairings (automorphisms) of one graph; that is, the pairing of Figure 1 is $2 \leftrightarrow 2$, $4 \leftrightarrow 4$, $6 \leftrightarrow 6$, $8 \leftrightarrow 8$ and $1 \leftrightarrow 3$, $3 \leftrightarrow 1$, $5 \leftrightarrow 7$, $7 \leftrightarrow 5$. (The matter of which points are equivalent and how to check all possible pairings is discussed in ref. 15.) In the example in Figure 1, the distance to the closest achiral object (d) also measures the distance to the nearest mirror-symmetric object, because the distance to, say, an object with inversion symmetry is larger. We now examine Figure 2, which illustrates other possibilities.

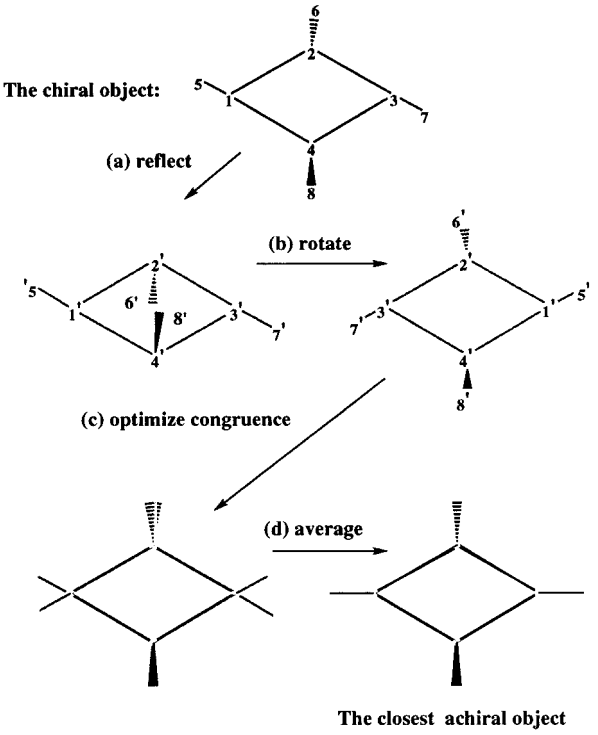

FIGURE 1. The use of pose estimation methods for the calculation of the closest achiral object. (a) Formation of the enantiomer by reflection through an arbitrary plane (in this case, the plane of the quadrangle). (b) Rotation, such that the congruence (c) with the original object is optimal (in this case, rotation by π radians through the 2′,4′ axis). (d) Averaging. Note the pairing of the points of the original object to its enantiomer: $1 \rightarrow 3'$, $2 \rightarrow 2'$, $3 \rightarrow 1'$, $4 \rightarrow 4'$, $5 \rightarrow 7'$, $6 \rightarrow 6'$, $7 \rightarrow 5'$, $8 \rightarrow 8'$.

Consider a box (Fig. 2) described by its vertices (the edges are drawn only to lead the eye). For all cases shown, the nearest projection plane is the plane that bisects the short edges, yet the nearest achiral objects are different, and are determined by

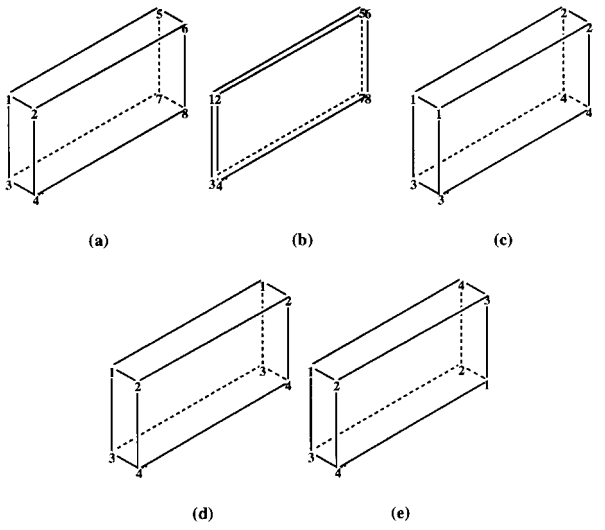

FIGURE 2. The four boxes (a, c–e) differ by color of vertices (denoted by different numbering), but have the same nearest projection plane, shown as a collapsed 2D box (b). For the case of the chiral box (a), object (b) is also the closest achiral object. Yet, for the achiral boxes (c–e), the closest achiral objects are, obviously, these objects themselves.

the different pairings (coloring) of the vertices. We begin with the case of a different color (i.e., vertex number) to each vertex (Fig. 2a). It is a chiral object, and the nearest achiral object to it is the ''planar'' box (Fig. 2b) that bisects (1,2);(3,4);(5,6);(7,8). S is then the distance (by MS) from this closest projection plane (which can be calculated by a simpler procedure[16]). Our next case is of an achiral box, shown in Figure 2c, for which the closest achiral object and the closest planar object are not the same objects: The closest achiral object is, of course, the 3D box itself, and the closest projection plane is the one that bisects the short edges of the box, which is also the plane of reflection—but this is not always necessarily so. As shown in Figure 2d, a different colored achiral box leads to a situation in which the nearest projection plane (the same as in Fig. 2c), is not the plane of reflection (which bisects the long edges). Finally, note that different coloring may result in different symmetry of the closest achiral object, such is the case in Figure 2e where achirality is due to inversion symmetry. In such cases naive application of a superpositioning procedure would lead to a wrong result, namely calculating the closest inversion-symmetric object instead. It is here that one is confronted with the need for an explicit procedure for the calculation of the closest reflection-symmetric object. Having clarified the problem, we now move on to its solution.

Solution by Reduction to the Problem of Fitting Two Sets of Points by C_2 Rotation

This problem is solved by reducing it to another problem, which at first glance does not seem to be easier; that is, fitting two sets of points by a c_2 rotation. The reduction is based on the fact that a reflection can be represented by an inversion, i, followed by a c_2 rotation, as illustrated in Figure 3. Thus, one searches for the best orientation of the reflection plane, σ, so as to minimize:

$$S(\sigma) = \frac{1}{N}\sum_{i=1}^{N}(p_j - \hat{p}_j)^2$$

but, equivalently, one may minimize:

$$\tilde{S}(\sigma) = \sum_{j=1}^{N}\left(p_j - \sigma(p_j^r)\right)^2$$

(cf. Fig. 4) where a point p_j is mapped either to its pair p_j^r or to itself ($p_j^r = p_j$) (note that each pair is counted twice and each singleton once). The reflection is then decomposed into an inversion, i,

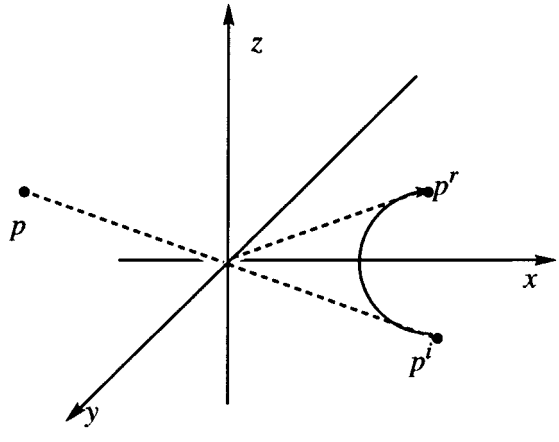

FIGURE 3. The representation of reflection by decomposition into inversion and c_2 rotation. Reflection through the y–z plane transforms p to p^r. Equivalently, the reflection can be decomposed to inversion ($p \rightarrow p^i$) and then rotation by π radians around the appropriate axis, in this case the x axis ($p^i \rightarrow p^r$).

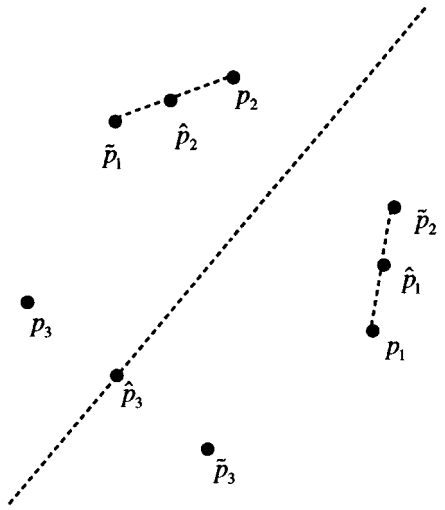

FIGURE 4. Equivalence of two sums. Three points (p_1, p_2, p_3) are part of an object deviating from the dotted line reflection symmetry. Points p_1 and p_2 are paired and point p_3 is a singleton. The reflected points are $(\tilde{p}_1, \tilde{p}_2, \tilde{p}_3)$ and the closest reflection symmetric points are $(\hat{p}_1, \hat{p}_2, \hat{p}_3)$. The contribution of these points to the (unnormalized) CSM (σ) value is $(p_1 - \hat{p}_1)^2 + (p_2 - \hat{p}_2)^2 + (p_3 - \hat{p}_3)^2$, which is exactly one fourth of the sum $(p_1 - \tilde{p}_2)^2 + (p_2 - \tilde{p}_1)^2 + (p_3 - \tilde{p}_3)^2$.

through the mass center and a c_2 operation:

$$\tilde{S}(\sigma) = \sum_{j=1}^{N} \left(p_j - c_2\left(\boldsymbol{i}(p_j^r)\right)\right)^2 \qquad (2)$$

Because the inversion point is known to coincide with the center of mass,[5] the problem has been reduced to finding the best c_2 rotation between the two sets:

$$\{p_j\}, \quad j = 1..N \qquad \text{and} \qquad \left\{\boldsymbol{i}(p_j^r)\right\}, \quad j = 1..N$$

The closest C_2-symmetric object can be obtained in the same manner by minimizing:

$$\tilde{S}(c_2) = \sum_{j=1}^{N} \left(p_j - c_2(p_j^r)\right)^2 \qquad (3)$$

Thus, the problem of finding the nearest reflection-symmetric object and the nearest C_2-symmetric object is reduced to finding the best c_2 rotation. We use the quaternion representation of rotations,[17] already used by Horn for the pose estimation problem,[13] to develop the closed-form solution for the best c_2 rotation. As this representation is not very common, we provide a brief review of the elements necessary for our application in the Appendix. In what follows, we use results from the Appendix, and the relevant equations are denoted with an A.

Recalling that one searches for the optimal c_2 rotation so as to minimize eq. (3), we first expand it, noting that:

$$\left(c_2(p_j^r)\right)^2 = (p_j^r)^2$$

thus:

$$\tilde{S}(c_2) = \sum_i p_{i,l}^2 + \sum_i p_{i,r}^2 - 2\sum_i p_{i,l} \cdot c_2(p_{i,r}) \qquad (4)$$

The first two sums are constant (by the normalization we imposed):

$$\sum_{j=1}^{N} p_j^2 = \sum_{j=1}^{N} (p_j^r)^2 = N$$

therefore, equivalently, one may maximize:

$$\phi(c_2) = \sum_{j=1}^{N} p_j \cdot c_2(p_j) \qquad (5a)$$

In the quaternion representation this may be written as:

$$\phi(q) = \sum_{j=1}^{N} p_j \cdot (q p_j^r q^*) \qquad (5b)$$

where q is the quaternion associated with the c_2 rotation. Using eq. (A17), we obtain:

$$\phi(q) = \sum_{j=1}^{N} (q p_j^r) \cdot (p_j q) \qquad (6)$$

In the quaternion matrix–vector form we have:

$$\phi(q) = \sum_j \left(\bar{\mathbf{P}}_j^r \mathbf{q}\right)^t \cdot (\mathbf{P}_j \mathbf{q}) = \sum_i \mathbf{q}^t \bar{\mathbf{P}}_j^{r\,t} \mathbf{P}_j \mathbf{q}$$

$$= \mathbf{q}^t \left(\sum_j \bar{\mathbf{P}}_j^{r\,t} \mathbf{P}_j \right) \mathbf{q} \qquad (7)$$

Using eqs. (A4) and (A5), the (symmetric) matrix:

$$\sum_j \bar{\mathbf{P}}_j^{r\,t} \mathbf{P}_j$$

is calculated:

$$\sum_j \bar{\mathbf{P}}_j^{r\,\mathrm{t}} \mathbf{P}_j = \begin{bmatrix} S_{xx}+S_{yy}+S_{zz} & S_{yz}-S_{zy} & S_{zx}-S_{xz} & S_{xy}-S_{yx} \\ S_{yz}-S_{zy} & S_{xx}-S_{yy}-S_{zz} & S_{xy}+S_{yx} & S_{zx}+S_{xz} \\ S_{zx}-S_{xz} & S_{xy}+S_{yx} & -S_{xx}+S_{yy}-S_{zz} & S_{yz}+S_{zy} \\ S_{xy}-S_{yx} & S_{zx}+S_{xz} & S_{yz}+S_{zy} & -S_{xx}-S_{yy}+S_{zz} \end{bmatrix} \tag{8}$$

where:

$$S_{xx} = \sum_j x_j x_j^r, \qquad S_{xy} = \sum_j x_j y_j^r$$

and so forth (x_j, y_j, and z_j are the coordinates of the point p_j). To simplify the calculation, it is convenient to introduce the *pairs outer product matrix*:

$$\mathbf{M} \equiv \sum_j p_j (p_j^r)^{\mathbf{t}} = \begin{bmatrix} S_{xx} & S_{xy} & S_{xz} \\ S_{yx} & S_{yy} & S_{yz} \\ S_{zx} & S_{zy} & S_{zz} \end{bmatrix} \tag{9}$$

this matrix takes a simple form if we change coordinates to $[\nu_i]$, the eigenbase of $\mathbf{M}$ (this is possible because $\mathbf{M}$ is symmetric). In this eigenbase, $\mathbf{M}$ and:

$$\sum_j \bar{\mathbf{P}}_j^{r\,\mathrm{t}} \mathbf{P}_j$$

are diagonal:

$$\mathbf{M} = \begin{bmatrix} s_x & 0 & 0 \\ 0 & s_y & 0 \\ 0 & 0 & s_z \end{bmatrix} \tag{10}$$

and:

$$\sum_j \bar{\mathbf{P}}_j^{r\,\mathrm{t}} \mathbf{P}_j = \begin{bmatrix} s_x+s_y+s_z & 0 & 0 & 0 \\ 0 & s_x-s_y-s_z & 0 & 0 \\ 0 & 0 & -s_x+s_y-s_z & 0 \\ 0 & 0 & 0 & -s_x-s_y+s_z \end{bmatrix} \tag{11}$$

substituting $\mathbf{q}^t = [0, \omega_x, \omega_y, \omega_z]$ [cf. Appendix A], we obtain the final form for $\phi(c_2)$:

$$\mathbf{q}^t \left(\sum_j \bar{\mathbf{P}}_j^{r\,\mathrm{t}} \mathbf{P}_j \right) \mathbf{q} = (s_x - s_y - s_z)\omega_x^2 + (-s_x + s_y - s_z)\omega_y^2 + (-s_x - s_y + s_z)\omega_z^2 \tag{12}$$

Assume, without loss of generality, that $s_x < s_y < s_z$, then $\phi(c_2)$ achieves maximal value when $\omega_x = 0$, $\omega_y = 0$, and $\omega_z = 1$.

Summary of minimization procedure. For each pairing of the points of the object, we calculate the pair's outer product matrix, $\mathbf{M}$, and diagonalize it. The axis of the optimal c_2 rotation is the eigenvector corresponding to the maximal eigenvalue of $\mathbf{M}$.

We also have at hand an explicit expression for $\tilde{S}(c_2)$ in terms of the eigenvalues of the outer product matrix:

$$\tilde{S}(c_2) = 2N + 2(s_x + s_y - s_z) \tag{13}$$

As the simplest confirmation of this expression one may note that, in the case of singleton mapping (i.e., each point is mapped onto itself), the distance from C_2-symmetry is equal to the sum-of-squares distance from the closest line, multiplied by 4:

$$\tilde{S}(c_2) = 2(s_x + s_y + s_z) + 2(s_x + s_y - s_z)$$

(as each point is paired to itself, the diagonal of the pairs outer product matrix $[s_x + s_y + s_z]$ is just

the points' sum of squares):

$$\sum_j p_j^2$$

By the normalization we impose:

$$\sum_j p_j = N \qquad \text{and} \qquad \tilde{S}(c_2) = 4(s_x + s_y),$$

equal to the sum of squares of the distances of the points from this line, $s_x + s_y$.[16]

In summary, we have derived a closed-form solution for the best c_2 rotation axis, which provides a robust method for the analysis of both C_2 and reflection symmetry. Although the derivation of the method has been based on the use of quaternions for the representation of the c_2 rotation, in the final form of the solution one need only diagonalize the pair's outer product matrix.

Appendix A: Quaternions

DEFINITION AND ELEMENTARY PROPERTIES

A quaternion can be thought of as a vector with four components or as a complex number with three different imaginary parts[13,17]:

$$q = q_0 + iq_x + jq_y + kq_z \tag{A1}$$

Multiplication of quaternions can be defined in terms of the products of their components, according to the following multiplication rules:

$$\begin{aligned} &i^2 = -1, \quad j^2 = -1, \quad k^2 = -1; \\ &ij = k, \quad jk = i, \quad ki = j; \qquad \text{and} \\ &ji = -k, \quad kj = -i, \quad ik = -j \end{aligned} \tag{A2}$$

Then, if:

$$r = r_0 + ir_x + jr_y + kr_z$$

we get:

$$\begin{aligned} rq = {} & r_0q_0 - r_xq_x - r_yq_y - r_zq_z \\ & + i(r_0q_x + r_xq_0 + r_yq_z - r_zq_y) \\ & + j(r_0q_y - r_xq_z + r_yq_0 + r_zq_x) \\ & + k(r_0q_z + r_xq_y - r_yq_x + r_zq_0) \end{aligned} \tag{A3}$$

in the general case, $rq \neq qr$.

Quaternions may be represented in vector form:

$$\left([\, q_0, q_x, q_y, q_z]^t \leftrightarrow q_0 + iq_x + jq_y + kq_z\right)$$

To mark which representation is used, we denote the vector representation in **bold** and the complex representation in *italic*. Their multiplication can be represented in matrix form (matrices are denoted by upper case letters and vectors by lower case letters):

$$rq = \begin{bmatrix} r_0 & -r_x & -r_y & -r_z \\ r_x & r_0 & -r_z & r_y \\ r_y & r_z & r_0 & -r_x \\ r_z & -r_y & r_x & r_0 \end{bmatrix} \begin{bmatrix} q_0 \\ q_x \\ q_y \\ q_z \end{bmatrix} \equiv \mathbf{Rq} \tag{A4}$$

Alternatively, the right-hand quaternion can be represented as a matrix multiplying the other quaternion from the left (by this manipulation we get an order exchange between the two). For convenience of notation, in the following derivations, we denote the left-hand quaternion by q and the right-hand quaternion by r:

$$qr = \begin{bmatrix} r_0 & -r_x & -r_y & -r_z \\ r_x & r_0 & r_z & -r_y \\ r_y & -r_z & r_0 & r_x \\ r_z & -r_y & -r_x & r_0 \end{bmatrix} \begin{bmatrix} q_0 \\ q_x \\ q_y \\ q_z \end{bmatrix} \equiv \overline{\mathbf{R}}\mathbf{q} \tag{A5}$$

Note that the matrices $\mathbf{R}$ and $\overline{\mathbf{R}}$ are orthogonal and that the sum of squares of each column (or row) is just the dot product $r \cdot r$ as we define in what follows, thus:

$$\mathbf{R}\mathbf{R}^{\mathbf{t}} = \overline{\mathbf{R}}\overline{\mathbf{R}}^{\mathbf{t}} = \left(r_0^2 + r_x^2 + r_y^2 + r_z^2\right)\mathbf{I} \tag{A6}$$

where $\mathbf{I}$ is the identity matrix.

DOT PRODUCTS OF QUATERNIONS

The dot product of quaternions is defined as:

$$r \cdot q = r_0q_0 + r_xq_x + r_yq_y + r_zq_z \tag{A7}$$

In vector form, the dot product is denoted as $r \cdot q = \mathbf{r}^{\mathbf{t}}\mathbf{q}$. The norm is defined as:

$$\|q\| = \sqrt{q \cdot q} \tag{A8}$$

If $q \cdot q = 1$, then q is a unit quaternion.

Taking the conjugate of a quaternion is defined as negating its imaginary part; thus:

$$q^* = q_0 - iq_x - jq_y - kq_z \tag{A9}$$

one can check that:

$$qq^* = q^*q = q_0^2 + q_x^2 + q_y^2 + q_z^2 = q \cdot q \tag{A10}$$

we conclude that a nonzero quaternion has an inverse $q^{-1} = q^*/q \cdot q$. In the case of a unit quaternion the inverse is simply the conjugate. Note that the matrix form of unit quaternions is simple as these matrices are orthonormal. The multiplication by the inverse quaternion is easily deduced as the inverse is just the transpose. Assuming multiplication from the left, we have:

$$q^{-1}r = q^*r = \mathbf{Q}^t\mathbf{r} \tag{A11}$$

and multiplication from the right:

$$rq^{-1} = rq^* = \overline{\mathbf{Q}}^t\mathbf{r} \tag{A12}$$

MORE USEFUL PROPERTIES

The orthogonality of the matrices representing (general) quaternions can be used to derive other useful properties of quaternions:

$$(qp) \cdot (qr) = (\mathbf{Qp})^t(\mathbf{Qr}) \tag{A13}$$

where the representation was changed into vector representation both inside and outside the parentheses. As:

$$(\mathbf{Qp})^t(\mathbf{Qr}) = \mathbf{p}^t\mathbf{Q}^t\mathbf{Qr} = \mathbf{p}^t(q \cdot q)\mathbf{Ir} = (q \cdot q)\mathbf{p}^t\mathbf{r} \tag{A14}$$

we conclude:

$$(qp) \cdot (qr) = (q \cdot q)(p \cdot r) \tag{A15}$$

The dot of the products is the product of the dots.

Another useful relation is derived as follows: Let b be a unit quaternion:

$$(ab) \cdot r = (\overline{\mathbf{B}}\mathbf{a})^t\mathbf{r} = \mathbf{a}^t\overline{\mathbf{B}}^t\mathbf{r} = a \cdot (rb^*) \tag{A16}$$

where the fact that b is a unit quaternion was used in the last equality. If we substitute qp for a and $q*$ for b we get:

$$(qpq^*) \cdot r = (qp) \cdot (rq) \tag{A17}$$

a result we use.

Vectors of the ordinary Euclidean space can be represented by purely imaginary quaternions:

$$r = ix + jy + kz \tag{A18}$$

Similarly, scalars can be represented by real quaternions. The matrices $\mathbf{R}$ and $\overline{\mathbf{R}}$ associated with pure imaginary quaternions are skew-symmetric. That is:

$$\mathbf{R}^t = -\overline{\mathbf{R}} \qquad \text{and} \qquad \mathbf{R} = -\overline{\mathbf{R}}^t \tag{A19}$$

UNIT QUATERNIONS AND ROTATIONS

It can be shown that unit quaternions may be used to represent rotations where the rotation operates on a vector by a conjugation; that is, the rotation of vector r "by q" is $r' = qrq^*$. One advantage of the quaternion representation of rotations is their explicit geometric interpretation: it can be shown that the quaternion associated with a rotation around the axis ω by an angle θ is:

$$\cos(\theta/2) + \sin(\theta/2)(i\omega_x + j\omega_y + k\omega_z), \tag{A20a}$$

or in succinct form:

$$\cos(\theta/2) + \sin(\theta/2)\omega \tag{A20b}$$

We use this feature to imply constraints on the rotations in a very straightforward way. Substituting π for θ, it is satisfying to note that the quaternion associated with a c_2 rotation is purely imaginary and fully parameterized by the axis of rotation ω. Last, note that the formulation of a rotation by conjugation takes a simpler form in the vector–matrix representation of the quaternion multiplication:

$$r' = qrq^* = \mathbf{Q}\overline{\mathbf{Q}}^t\mathbf{r} \tag{A21}$$

References

1. King, G. W.; Hainer, R. M.; Cross, P. C. J Chem Phys 1943, 11, 27.
2. Ray, B. S. Zeit Phys 1932, 78, 74.
3. (a) Avnir, D.; Katzenelson, O.; Keinan, S.; Pinsky, M.; Pinto, Y.; Salomon, Y.; Zabrodsky Hel-or, H. In: Rouvray, D. H.; Kirby, E., eds. Concepts in Chemistry: A Contemporary Challenge; Research Studies Press: Somerset, UK, 1997; Chapter 9; (b) Avnir, D.; Zabrodsky Hel-Or, H.; Mezey, P. G. Continuous symmetry and chirality measures. In: von Ragué Schleyer, P., ed. Encyclopedia of Computational Chemistry; John Wiley & Sons: Chichester, UK, 1998; p 2890.

4. (a) Kitaigorodskii, A. I. In: Organic Chemical Crystallography; Consultants Bureau: New York, 1961; Chapter 4; (b) Rassat, A. Comput Rend Acad Sci Paris II 1984, 299, 53; (c) Gilat, G. Chem Phys Lett 1985, 121, 9; (d) Maurani, J.; Mezey, P. G. Molec Phys 1990, 69, 97; (e) Mezey, P. G. Quantum Chem 1996, 27, 163; Mezey, P. G. Int J Quantum Chem 1997, 63, 39; (f) Mezey, P. G. In: Rouvray, D. H., ed. Fuzzy Logic in Chemistry; Academic Press: San Diego, CA; 1997, p 139; (g) Weinberg, N.; Mislow, K. J Math Chem 1993, 14, 427; (h) Ruch, E. Acc Chem Res 1972, 5, 49; (i) Kuzmin, V. E.; Stelmach, I. B.; Bekker, M. B.; Pozigun, D. V. J Phys Org Chem 1992, 5, 295; (j) Osipov, M. A.; Pickup, B. T.; Dunmur, D. A. Molec Phys 1995, 84, 1193; (k) Moreau, G. J Chem Inf Comput Sci 1997, 37, 929; (l) Raji, M.; Cosse-Barbi, A. C R Acad Paris 1997, 324b, 133.
5. Zabrodsky, H.; Peleg, S.; Avnir, D. J Am Chem Soc 1992, 114, 7843.
6. Zabrodsky, H.; Peleg, S.; Avnir, D. J Am Chem Soc 1995, 117, 462.
7. Zabrodsky, H.; Peleg, S.; Avnir, D. J Am Chem Soc 1993, 115, 8278. Erratum: 11656.
8. Zabrodsky, H.; Avnir, D. Adv Molec Struct Res 1995, 1, 1.
9. Some representative examples include: (a) Buch, V.; Gershgoren, E.; Zabrodsky, H.; Avnir, D. Chem Phys Lett 1995, 247, 149; (b) Pinto, Y.; Hel-Or, H. Z.; Avnir, D. J Chem Soc Faraday Trans 1996, 92, 2523; (c) Pinto, Y.; Salomon, Y.; Avnir, D. J Math Chem 1998, 23, 13; (d) Pinto, Y.; Fowler, P. W.; Mitchell, D.; Avnir, D. J Phys Chem 1998, 102, 5776.
10. Keinan, S.; Edelstein, J.; Plato, M.; Pinsky, M.; Avnir, D. Chem Phys Lett 1998, 298, 43; Keinan, S.; Avnir, D. Continuous symmetry measure as a tool in drug design. WATOC '96, Book of Abstracts.
11. Kabtch, W. Acta Crystallogr A 1976, 32, 922.
12. Arun, K. S.; Huang, T. S.; Blostein, S. D. IEEE Trans PAMI 1987, 9, 698.
13. Horn, B. K. P. J Opt Soc Am 1987, A4, 629.
14. Weinberg, N.; Mislow, K. J Math Chem 1995, 17, 35.
15. (a) Salomon, Y. Continuous Symmetry Measures: Algorithms for the Calculation of the Distance from Point Symmetries and the Measurement of the Distance from Translational Symmetry in Small Clusters; MSc Thesis, Hebrew University, Jerusalem, 1998; (b) Salomon, Y.; Avnir, D. J Math Chem, submitted, 1997. In passing, we note that the equivalence between the points of the graph $G(V, E)$ (V is the set of points $p_1 \ldots p_N$ and E is the set of edges connecting them) may be defined recursively as follows: A mapping of p_j to p_k is proper if they have the same number of neighbors and each neighbor of p_j is properly mapped to a neighbor of p_k.
16. Schomaker, V.; Waser, J. Acta Crystallogr 1959, 12, 600.
17. du Val, P. Homographies, Quaternions and Rotations; Clarendon Press: Oxford, UK, 1964.